

Remote estimation of leaf area index and green leaf biomass in maize canopies

Anatoly A. Gitelson,^{1,2,4} Andrés Viña,^{1,2} Timothy J. Arkebauer,³ Donald C. Rundquist,^{1,2} Galina Keydan,¹ and Bryan Leavitt¹

Received 14 October 2002; revised 26 December 2002; accepted 3 February 2003; published 13 March 2003.

[1] Leaf area index (LAI) is an important variable for climate modeling, estimates of primary production, agricultural yield forecasting, and many other diverse studies. Remote sensing provides a considerable potential for estimating LAI at local to regional and global scales. Several spectral vegetation indices have been proposed, but their capacity to estimate LAI is highly reduced at moderate-to-high LAI. In this paper, we propose a technique to estimate LAI and green leaf biomass remotely using reflectances in two spectral channels either in the green around 550 nm, or at the red edge near 700 nm, and in the NIR (beyond 750 nm). The technique was tested in agricultural fields under a maize canopy, and proved suitable for accurate estimation of LAI ranging from 0 to more than 6. *INDEX TERMS:* 1640 Global Change: Remote sensing; 1694 Global Change: Instruments and techniques; 1699 Global Change: General or miscellaneous. *Citation:* Gitelson, A. A., A. Viña, T. J. Arkebauer, D. C. Rundquist, G. Keydan, and B. Leavitt, Remote estimation of leaf area index and green leaf biomass in maize canopies, *Geophys. Res. Lett.*, 30(5), 1248, doi:10.1029/2002GL016450, 2003.

1. Introduction

[2] One of the key variables required in estimating primary production and in global climate studies is leaf area index (LAI), the ratio of one-sided green leaf area to ground area. Remote estimations of LAI at regional and global scales might be performed mainly using transforms of spectral reflectance, called vegetation indices [e.g., *Rouse et al.*, 1974]. A physically based algorithm for estimation of LAI from Normalized Difference Vegetation Index (NDVI) observations was developed [e.g., *Myneni et al.*, 1997]. As the authors noted, “the algorithm must be viewed within a framework dominated largely by practical consideration and to a lesser extent by accuracy”. The relationship between NDVI and LAI is essentially non-linear and exhibits significant variation among various cover types. When LAI exceeds 2, NDVI is generally insensitive to LAI, not only in forest canopies with a dense understory, but also in grasses, cereal crops, and broadleaf crops [see Figure 5 in *Myneni et*

al., 1997]. The linkage between surface reflectance and LAI is not straightforward and at the present time it appears that no satisfactory algorithm exists for remote retrieval of moderate-to-high LAI > 2.

[3] In this paper we present a new approach to accurately estimate LAI and green leaf biomass using reflectance in the green and red edge regions of the electromagnetic spectrum. We demonstrate the advantage of this approach over the traditional NDVI for maize canopies.

2. Methods

[4] A pilot study was conducted in 2001 to examine the relationship between remotely measured reflectance and LAI for a maize canopy. The project was carried out in two large irrigated production fields (each 65 ha). Within each of the two study sites, six small (20 m × 20 m) plot areas were established. These intensive measurement zones (IMZ) represented all major occurrences of soil and crop production zones within each site.

[5] Spectral measurements were made using two hyper-spectral radiometers mounted on “Goliath”, an all-terrain sensor platform [*Rundquist et al.*, 2001]. Six plots were established per field for these measurements, each with six randomly selected sampling points. A dual-fiber system, with two inter-calibrated Ocean Optics USB2000 radiometers, was used to collect data in the range 400–900 nm with a spectral resolution of about 1.5 nm. Radiometer #1, equipped with a 25° field-of-view optical fiber was pointed downward to measure the upwelling radiance of maize (L_{λ}^{maize}). The position of the radiometer above the canopy was kept constant throughout the growing season (i.e. around 5.4 m), yielding a sampling area with a diameter of around 2.4 m. Radiometer #2, equipped with an optical fiber and cosine diffuser (yielding a hemispherical field of view), was pointed upward to simultaneously measure incident irradiance (E_{λ}^{inc}). To match their transfer functions, inter-calibration of the radiometers was accomplished by measuring the upwelling radiance (L_{λ}^{cal}) of a white Spectralon reflectance standard (Labsphere, Inc., North Sutton, NH) simultaneously with incident irradiance (E_{λ}^{cal}). To mitigate the impact of solar elevation on radiometer intercalibration, the anisotropic reflectance from the calibration target was corrected in accord with *Jackson et al.* [1992]. Percent reflectance (ρ_{λ}) was computed as:

$$\rho_{\lambda} = (L_{\lambda}^{maize} / E_{\lambda}^{inc}) (E_{\lambda}^{cal} / L_{\lambda}^{cal}) * 100 * \rho_{\lambda}^{cal} \quad (1)$$

Here ρ_{λ}^{cal} is the reflectance of the Spectralon panel linearly interpolated to match the band centers of each radiometer.

¹Center for Advanced Land Management Information Technologies (CALMIT), University of Nebraska-Lincoln, Lincoln, Nebraska, USA.

²School of Natural Resource Sciences, University of Nebraska-Lincoln, Lincoln, Nebraska, USA.

³Department of Agronomy, University of Nebraska-Lincoln, Lincoln, Nebraska, USA.

⁴Also at J. Blaustein Institute for Desert Research, Ben-Gurion University of the Negev, Beer-Sheva, Israel.

Table 1. Average Digital Numbers in Two HYPERION^a Images (bands 18 to 21–530–560 nm) of the IMZ Sampling Areas and the Areas Sampled From the “Goliath” Platform

	Date	Goliath Sample Area	IMZ	T-test	P-value
Field 1	8/13/01	1556.25 (11.53)	1547.12 (6.52)	1.69	0.12
	8/29/01	1568.37 (5.89)	1566.42 (6.74)	0.54	0.60
Field 2	8/13/01	1523.83 (18.97)	1522.71 (15.24)	0.11	0.91
	8/29/01	1545.33 (15.37)	1544.75 (6.54)	0.09 ^b	0.93

Numbers in parentheses correspond to standard deviations. T-test values and P-values correspond to the comparison of means of “Goliath” sample areas and IMZ sampling areas ($n = 6$).

^aHYPERION is a hyperspectral imager onboard NASA’s Earth Observing - 1 satellite, with 220 spectral bands (from 0.4 to 2.5 μm) and 30 m/pixel.

^bTwo sample T-test assuming unequal variances.

[6] One critical issue with regard to the dual-fiber approach is that the transfer functions of both radiometers must be identical. We tested our Ocean Optics instruments under laboratory conditions; over a four-hour period the standard deviations of the ratio of the two transfer functions did not exceed 0.004.

[7] Data were collected with the sensors configured to take 15 simultaneous upwelling radiance and downwelling irradiance measurements, which were internally averaged and stored as a single data file. Radiometric data were collected close to solar noon (between 11am and 1pm), when diurnal changes in solar zenith angle are minimal. Measurements took about 3–4 minutes per plot and about 20 minutes per field. The two radiometers were inter-calibrated immediately before and immediately after measurement in each field. Eighteen campaigns were carried out from the beginning of June to the beginning of October 2001.

[8] NDVI was calculated as $(\rho_{\text{NIR}} - \rho_{\text{red}})/(\rho_{\text{NIR}} + \rho_{\text{red}})$ where $\rho_{\text{NIR}} = \rho_{840-880}$, $\rho_{\text{red}} = \rho_{630-690}$ are reflectance values in spectral channels of the Moderate Resolution Imaging Spectroradiometer (MODIS; onboard NASA’s Terra satellite). Visible Atmospherically Resistant Indices [Gitelson *et al.*, 2002a] were calculated as $\text{VARI}_{\text{Green}} = (\rho_{\text{green}} - \rho_{\text{red}})/(\rho_{\text{green}} + \rho_{\text{red}} - \rho_{\text{blue}})$ and $\text{VARI}_{\text{RedEdge}} = (\rho_{\text{RedEdge}} - 1.7 * \rho_{\text{red}} - 0.7 * \rho_{\text{blue}})/(\rho_{\text{RedEdge}} + 2.3 * \rho_{\text{red}} - 1.3 * \rho_{\text{blue}})$. VARI and indices proposed in this work were calculated in spectral channels of MODIS $\rho_{\text{blue}} = \rho_{460-480}$, $\rho_{\text{green}} = \rho_{545-565}$, $\rho_{\text{red}} = \rho_{660-680}$, and of the Medium Resolution Imaging Spectrometer (MERIS; onboard the polar orbiting Envisat Earth Observation Satellite): $\rho_{\text{RedEdge}} = \rho_{700-710}$.

[9] Plant populations were determined (by counting plants) for each IMZ. On each sampling date, plants from a 1m length of either of two rows were collected and total number of plants recorded. Collection rows were alternated on successive dates to minimize edge effects on subsequent plant growth. Plants were transported on ice to the laboratory. In the lab, plants were dissected into green leaves, dead leaves, stems, and reproductive organs. The green leaves were run through an area meter (Model LI-3100, Li-Cor, Inc., Lincoln NE) and the leaf area per plant was determined. For each IMZ, the green leaf area per plant was multiplied by the plant population ($\# \text{ plants m}^{-2}$) to obtain a LAI. LAI at the six IMZs were averaged to obtain a site-level value. All plant parts were dried to constant weight in a 70 °C dryer. Site-level green leaf biomass was then calculated in a manner analogous to LAI.

[10] LAI ranged from 0 to more than 6. Standard deviations of the destructive measurements of LAI ranged from 0.05 at the beginning of the growing season, at day of the year (DOY) 163, to 0.48 before the peak of maximum LAI (DOY 180).

[11] Field heterogeneity was tested using two HYPERION (Hyperspectral Imager onboard Earth Observing-1 satellite) images acquired on August 13 and 29, 2001 with a spatial resolution of 30 m/pixel. The average digital numbers of the areas where destructive sampling of LAI was carried out (IMZs) were compared against the average digital numbers within the areas where reflectance was measured from the “Goliath” platform, and no statistically significant differences were obtained (Table 1). Thus, test sites, where reflectance measurements were conducted, were representative of those where destructive sampling of LAI occurred.

3. Results and Discussion

[12] NDVI was sensitive to LAI in the beginning of the growing season (LAI changed from 0 to 1.2; Figure 1A). NDVI reached maximal values around 0.9 at DOY 190 and then remained virtually invariant between DOY 210 and 233. The relationship between NDVI and LAI was essentially non-linear (Figure 1-insert). Other indices used for estimation of vegetation status (e.g., SAVI, PVI, ARVI, GARI) also showed low sensitivity to LAI exceeding 1.5 (data not shown).

[13] Temporal behavior of both $\text{VARI}_{\text{Green}}$ and $\text{VARI}_{\text{RedEdge}}$ were quite different from that of NDVI (Figure 1). VARI followed LAI throughout the whole range of LAI variation. It had a pronounced peak at DOY 190 when greenness of maize was maximal, and then decreased significantly reaching a plateau at DOY 210. When tassels (i.e. flowering) appeared, reflectance of the canopy in visible spectrum increased; the increase was especially pronounced in the red and the red edge ranges. Increase in red reflectance was about 50% higher than in the green and about 10% higher than in the red edge (data not shown). Thus, appearance of tassels led to decrease in both $\text{VARI}_{\text{Green}}$ and $\text{VARI}_{\text{RedEdge}}$.

[14] The relationship between VARI and LAI had two distinct stages (Figure 2): (i) an increase in VARI was associated with an increase in LAI between 0 and 6 until

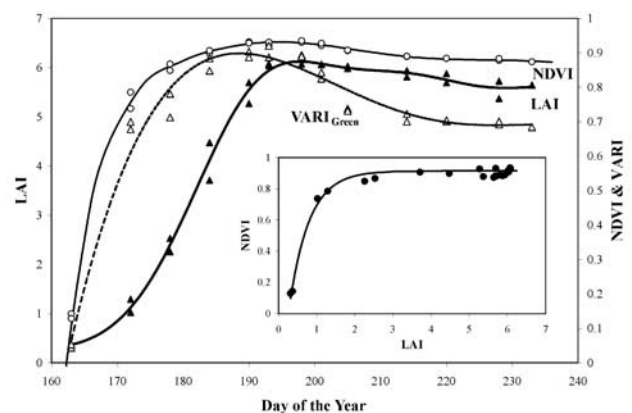


Figure 1. Temporal behavior of maize LAI, VARI and NDVI at two sites. In insert: NDVI plotted versus LAI. VARI was adjusted to match NDVI scale.

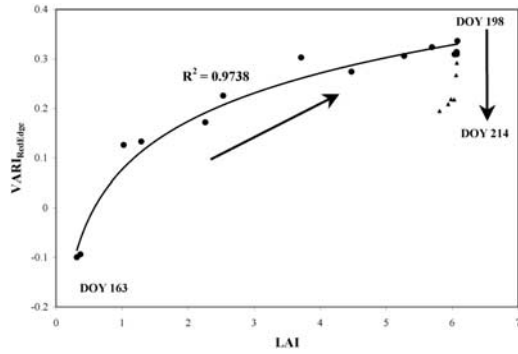


Figure 2. Visible Atmospherically Resistant Index ($VARI_{RedEdge}$) vs. LAI. The arrows show the direction of the progression of the growing season. Best-fit function was established between day of the year (DOY) 163 and 198 before tassels appeared.

tasseling occurred (DOY 163 to 198); and (ii) a decrease in VARI when tassels appeared, while LAI remained virtually invariant (DOY 198 to 214). In the first stage the relationship was logarithmic (a coefficient of determination $r^2 = 0.97$) with significant sensitivity of the index to LAI ranged from 0 to 6. The decrease in VARI as a result of tassels appearing makes the relationship weaker, nevertheless, VARI accounted for 85% of LAI variation.

[15] The derivative of vegetation reflectance, ρ , with respect to wavelength ($d\rho/d\lambda$) is common to all vegetation indices and is indicative of the abundance and activity of absorbers in leaves. For optically dense canopy, $d\rho/d\lambda = F(\alpha_\lambda, \chi, LAI, R)$, where α_λ is absorber-specific absorption coefficient, χ is absorber concentration per unit leaf area, and R is a response function that describes the effect of canopy architecture [Myneni *et al.*, 1995]. Thus, vegetation indices are the convolution of pigment concentration in the leaves ($\alpha_\lambda \chi$), LAI, and response function R . This was the theoretical background sought for satellite remote sensing of vegetation biochemical constituents, including LAI.

[16] In the red spectral range used for calculating vegetation indices such as NDVI, SAVI, ARVI and Simple Ratio, (ρ_{NIR}/ρ_{red}), among others, the specific absorption coefficient of chlorophylls (α_{red}) is high [e.g. Lichtenthaler, 1987] and the depth of light penetration into the leaf is low [e.g. Kumar and Silva, 1973]. As a result, even low amounts of pigments or small LAI are sufficient to saturate absorption [Kanemasu, 1974; Buschmann and Nagel, 1993; Gitelson *et al.*, 2002a, 2002b]. This explains the essentially non-linear behavior of NDVI as a function of LAI (insert in Figure 1), since the index becomes non-sensitive at LAI values higher than 2.

[17] Specific absorption coefficients of chlorophylls in the green and red edge spectral regions are much smaller than in the red region (α_{green} and $\alpha_{RedEdge}$ are around 2–5% of α_{red} [Lichtenthaler, 1987]). Thus, in these spectral ranges absorption does not saturate at moderate to high chlorophyll contents [e.g. Thomas and Gaussman, 1977; Buschmann and Nagel, 1993; Gitelson and Merzlyak, 1994; Gitelson *et al.*, 1996; Yoder and Waring, 1994]. On the other hand, in these spectral regions light penetrates into the leaf deeper than in the red, therefore, absorption of light is sufficient to provide high sensitivity of reflectance to chlorophyll content. This was the background sought for chlorophyll

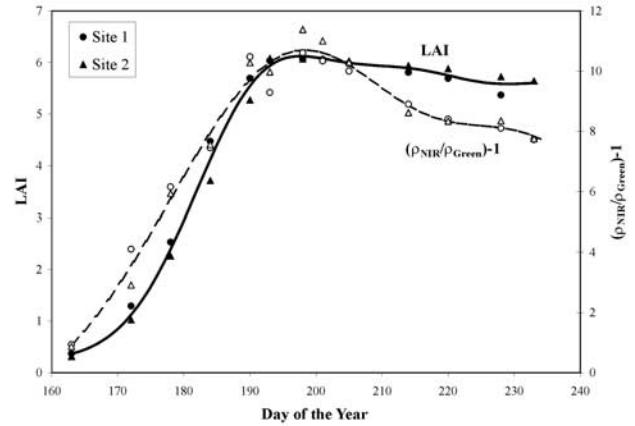


Figure 3. Temporal behavior of maize LAI and the proposed index $[(\rho_{NIR}/\rho_{Green}) - 1]$.

estimation at leaf level. The index $[(\rho_{NIR}/\rho_\lambda) - 1]$ in spectral ranges (λ) in the green and the red edge was found to be linearly proportional to leaf chlorophyll content [Gitelson and Merzlyak, 1994; Gitelson *et al.*, 2003].

[18] Thus, we hypothesized that at community level the indices $[(\rho_{NIR}/\rho_{Green}) - 1]$ and $[(\rho_{NIR}/\rho_{RedEdge}) - 1]$ relate to total pigment concentration in the canopy ($\chi * LAI$). This assumption was valid for maize with LAI ranging from 0 to 6 (Figure 3). Before tassels appeared, close linear relation-

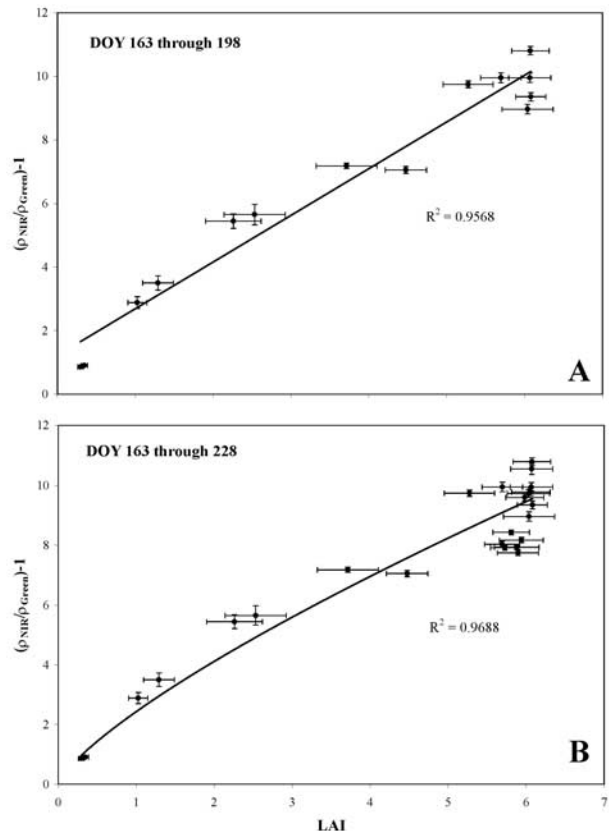


Figure 4. The proposed index $[(\rho_{NIR}/\rho_{green}) - 1]$, plotted vs. LAI for the data (A) between day of the year (DOY) 163 and 198 before tassels appeared; (B) obtained over the whole growing season. Error bars correspond to two standard errors.

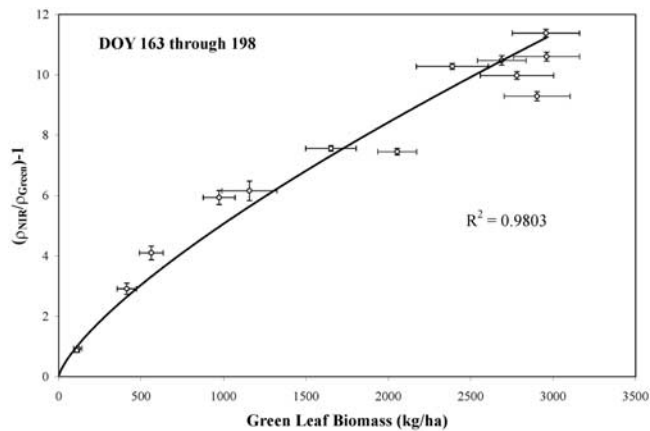


Figure 5. The index $[(\rho_{\text{NIR}}/\rho_{\text{Green}}) - 1]$ plotted vs. green leaf biomass for the data between day of the year (DOY) 163 and 198 before tassels appeared.

ships ($r^2 > 0.95$) between LAI and both indices were established (Figure 4A; $r^2 = 0.96 \tan [(\rho_{\text{NIR}}/\rho_{\text{RedEdge}}) - 1]$). When tassels appeared, LAI remained almost the same, while the indices decreased following a significant increase in reflectance, particularly in the red and red edge regions. Nevertheless, for the entire growing season, the indices described more than 95% of LAI variability (Figure 4B). Newly proposed indices were also closely related to green leaf biomass (Figure 5).

[19] As it was mentioned, the indices $[(\rho_{\text{NIR}}/\rho_{\text{Green}}) - 1]$ and $[(\rho_{\text{NIR}}/\rho_{\text{RedEdge}}) - 1]$ depend not only on LAI but also on chlorophyll concentration per unit leaf area. From DOY 164 to 220, the coefficient of variation of chlorophyll content, measured in upper canopy green leaves, was less than 11%, while coefficients of variation of both LAI and green leaf biomass were 46% and 49%, respectively. Thus, the observed variation of the indices was governed mainly by LAI.

[20] The approach was validated by comparing the predicted against the measured LAI. Linear models $[(\rho_{\text{NIR}}/\rho_{\text{Green}}) - 1]$ and $[(\rho_{\text{NIR}}/\rho_{\text{RedEdge}}) - 1]$ vs. LAI developed from measurements at site 1 were compared against LAI measurements at site 2. The Root Mean Square Error of LAI prediction was less than 0.61.

4. Conclusions

[21] Close relationships were found between newly proposed indices, $[(\rho_{\text{NIR}}/\rho_{\text{Green}}) - 1]$ and $[(\rho_{\text{NIR}}/\rho_{\text{RedEdge}}) - 1]$, and LAI (ranging from 0 to more than 6), as well as green leaf biomass (0 to 3500 kg/ha). These indices and recently proposed VARI, were indicative of both the phenological stages of vegetation during the growing season and of flowering (the appearance of tassels). More work is needed to study the sensitivity of the indices to LAI in other vegetation types as well as the spectral properties of the tassels and their influence on total canopy reflectance.

[22] **Acknowledgments.** This research was supported partially by the U.S. Department of Energy: (a) EPSCoR program, Grant No. DE-FG-02-00ER45827 and (b) Office of Science (BER), Grant No. DE-FG03-00ER62996. We acknowledge the use of facilities and equipment provided by the Center for Advanced Land Management Information Technologies (CALMIT), University of Nebraska-Lincoln. We also wish to thank Rick Perk, Jared Burkholder, and Jeff Moon for assistance with data collection. This paper has been assigned Journal Series No. 13977, Agricultural Research Division, University of Nebraska-Lincoln.

References

- Buschmann, C., and E. Nagel, In vivo spectroscopy and internal optics of leaves as basis for remote sensing of vegetation, *Int. J. Remote Sens.*, 14, 711–722, 1993.
- Gitelson, A. A., and M. N. Merzlyak, Quantitative estimation of chlorophyll-a using reflectance spectra: Experiments with autumn chestnut and maple leaves, *Photochem. Photobiol.*, 22, 247–252, 1994.
- Gitelson, A. A., Y. J. Kaufman, and M. N. Merzlyak, Use of green channel in remote sensing of global vegetation from EOS-MODIS, *Remote Sens. Environ.*, 58, 289–298, 1996.
- Gitelson, A. A., Y. J. Kaufman, R. Stark, and D. Rundquist, Novel algorithms for remote estimation of vegetation fraction, *Remote Sens. Environ.*, 80, 76–87, 2002a.
- Gitelson, A. A., Y. Zur, O. B. Chivkunova, and M. N. Merzlyak, Assessing carotenoid content in plant leaves with reflectance spectroscopy, *Photochem. Photobiol.*, 75, 272–281, 2002b.
- Gitelson, A. A., U. Gritz, and M. N. Merzlyak, Relationships between leaf chlorophyll content and spectral reflectance and algorithms for non-destructive chlorophyll assessment in higher plant leaves, *J. Plant Physiol.*, 160, 271–282, 2003.
- Jackson, R. D., T. R. Clarke, and M. S. Moran, Bidirectional calibration results for 11 Spectralon and 16 BaSO4 reference reflectance panels, *Remote Sens. Environ.*, 40, 231–239, 1992.
- Kanemasu, E. T., Seasonal canopy reflectance patterns of wheat, sorghum, and soybean, *Remote Sens. Environ.*, 3, 43–47, 1974.
- Kumar, R., and L. Silva, Light ray tracing through a leaf cross section, *Appl. Opt.*, 12, 2950–2954, 1973.
- Lichtenthaler, H. K., Chlorophylls and carotenoids: Pigments of photosynthetic biomembranes, *Methods Enzymology*, 148, 350–382, 1987.
- Myneni, R. B., F. G. Hall, P. J. Sellers, and A. L. Marshak, The interpretation of spectral vegetation indexes, *IEEE Trans. Geosci. Remote Sens.*, 33, 481–486, 1995.
- Myneni, R. B., R. R. Nemani, and S. W. Running, Estimation of global leaf area index and absorbed PAR using radiative transfer models, *IEEE Trans. Geosci. Remote Sens.*, 35, 1380–1393, 1997.
- Rouse, J. W., R. H. Haas Jr., J. A. Schell, and D. W. Deering, Monitoring vegetation systems in the Great Plains with ERTS, NASA SP-351, *Third ERTS-1 Symposium*, vol. 1, pp. 309–317, NASA, Washington, D. C., 1974.
- Rundquist, D., A. A. Gitelson, D. Derry, J. Ramirez, R. Stark, and G. Keydan, Remote estimation of vegetation fraction in corn canopies, in *Proceedings of the Third European Conference on Precision Agriculture*, vol. 1, edited by G. Grenier and S. Blackmore, pp. 301–306, 2001.
- Thomas, J. R., and H. W. Gaussman, Leaf reflectance vs. leaf chlorophyll and carotenoid concentration for eight crops, *Agron. J.*, 69, 799–802, 1977.
- Yoder, B. J., and R. H. Waring, The normalized difference vegetation index of small Douglas-fir canopies with varying chlorophyll concentrations, *Remote Sens. Environ.*, 49, 81–91, 1994.

T. J. Arkebauer, Department of Agronomy, University of Nebraska-Lincoln, 279 Plant Science, Lincoln, NE 68583, USA. (tarkebau@unlnotes.unl.edu)

A. A. Gitelson, G. Keydan, B. Leavitt, D. C. Rundquist, and A. Viña, Center for Advanced Land Management Information Technologies (CALMIT), University of Nebraska-Lincoln, 113 Nebraska Hall, Lincoln, NE 68588-0517, USA. (gitelson@calmit.unl.edu; keydan@calmit.unl.edu; bleavitt@calmit.unl.edu; drundquist1@unl.edu; avina@calmit.unl.edu)